HHS Public Access

Author manuscript

Neurobiol Dis. Author manuscript; available in PMC 2022 October 01.

Published in final edited form as:

Neurobiol Dis. 2021 October ; 158: 105456. doi:10.1016/j.nbd.2021.105456.

A novel role for the ADHD risk gene *latrophilin-3* in learning and memory in *Lphn3* knockout rats

Samantha L. Regan[1], **Emily M. Pitzer**[1], **Jillian R. Hufgard**, **Chiho Sugimoto**, **Michael T. Williams**, **Charles V. Vorhees**[*]

Dept. of Pediatrics, University of Cincinnati College of Medicine, and Division of Neurology, Cincinnati Children's Research Foundation, Cincinnati, OH, 45229 USA

Abstract

Latrophilins (LPHNs) are adhesion G protein-coupled receptors with three isoforms but only LPHN3 is brain specific (caudate, prefrontal cortex, dentate, amygdala, and cerebellum). Variants of *LPHN3* are associated with ADHD. Null mutations of *Lphn3* in rat, mouse, zebrafish, and *Drosophila* result in hyperactivity, but its role in learning and memory (L&M) is largely unknown. Using our *Lphn3* knockout (KO) rats we examined the cognitive abilities, long-term potentiation (LTP) in CA1, NMDA receptor expression, and neurohistology from heterozygous breeding pairs. KO rats were impaired in egocentric L&M in the Cincinnati water maze, spatial L&M and cognitive flexibility in the Morris water maze (MWM), with no effects on conditioned freezing, novel object recognition, or temporal order recognition. KO-associated locomotor hyperactivity had no effect on swim speed. KO rats had reduced early-LTP but not late-LTP and had reduced hippocampal NMDA-NR1 expression. In a second experiment, KO rats responded to a light prepulse prior to an acoustic startle pulse, reflecting visual signal detection. In a third experiment, KO rats given extra MWM pretraining and hidden platform overtraining showed no evidence of reaching WT rats' levels of learning. Nissl histology revealed no structural abnormalities in KO rats. LPHN3 has a selective effect on egocentric and allocentric L&M without effects on conditioned freezing or recognition memory.

[*]Corresponding author at: Div. of Neurology (MLC 7044), Cincinnati Children's Research Foundation, 3333 Burnet Ave., Cincinnati, OH 45229, USA. charles.vorhees@cchmc.org.

[1]These authors contributed equally to this work.

Author Contributions

S.L. Regan, E.M. Pitzer, J.R. Hufgard, and C. Sugimoto bred, genotyped, and did the behavioral testing of *Lphn3* KO rats and their WT littermates. E.M. Pitzer and S.L. Regan conducted the western analyses and LTP studies. M.T. Williams did the statistical analyses. E.M. Pitzer, S.L. Regan and C.V. Vorhees graphed the data. E.M. Pitzer and S.L. Regan drafted the manuscript and M.T. Williams and C.V. Vorhees edited the manuscript to its final form. C.V. Vorhees is PI of the *Lphn3* project and M.T. Williams is Co-PI.

Author Credit Statement

Dr. Regan collected and analyzed the data for about half the data presented and created the second draft of the manuscript. Dr. Pitzer collected some of the data and created the first draft of the manuscript. Dr. Hufgard collected the other half of the data presented. Ms. Sugimoto assisted in collecting the data. Drs. Williams and Vorhees designed the experiments, Dr. Williams oversaw the statistical analyses, and both graphed, interpreted, and revised the manuscript to its final form.

Disclosure: Dr. Vorhees declares no conflict of interest. He has served on the Scientific Advisory Committees on Chemicals for the U.S. Environmental Protection Agency, and on a Scientific Advisory Committee on Artificial Food Colors and Children's Behavior for the California Environmental Protection Agency, Office of Environmental Health Hazard Assessment.

Drs. Williams, Hufgard, Regan, and Pitzer, and Ms. Sugimoto declare no conflicts of interest regarding this research.

Keywords

Lphn3; *Adgrl-3*; *Lphn3* knockout rat; cognition; long-term potentiation; spatial learning and memory; egocentric learning; novel object recognition

Introduction

Latrophilin-3 (LPHN-3) is a member of the LPHN sub-family of adhesion G protein-coupled receptors (aGPCRs) whose role in learning and memory (L&M) is largely unknown. LPHNs bind to neurexins [1, 2], tenuerins (TEN3) [3], and fibronectin leucine rich transmembrane proteins (FLRT3) [1, 2]. The N-terminal contains adhesion motifs, an autoproteolysis GAIN domain, and a 7-transmembrane C-terminal [4]. The GAIN domain has a GPS auto-cleavage motif and a $G\alpha_{q/11}$ domain that activates phospholipase C mobilizing intracellular Ca^{2+} and neurotransmitter release [5].

There are three LPHN isoforms. LPHN1 is the receptor for α-latrotoxin in black widow spider venom (*Latrodectus mactans*) [6–8] where binding elicits GABA exocytosis [9–11]. LPHN2 is in brain, liver, and lung [12]. LPHN3 is brain-specific [13] and located in prefrontal cortex (PFC), caudate, hippocampus, amygdala, and cerebellum [14]. When LPHN3 binds to FLRT3 it regulates hippocampal glutamatergic pyramidal neuron density [2, 15–17]. When LPHN3 binds to both FLRT3 and TEN3 it regulates synaptic activation in CA1 pyramidal neurons in S. oriens and S. radiatum, and deletion of LPHN3 downregulates Schaffer collateral activity [18]. *LPHN3* genetic variants are associated with attention-deficit hyperactivity disorder (ADHD) [14, 19–23], Variants of *LPHN3* increased the risk of ADHD by 1.2-fold and were associated with symptom severity and medication response. The association was also found in North American, European, Spanish, Korean, and Chinese patients [22, 24–26]. Twenty-one *LPHN3* SNP variants are associated with ADHD [27] and with response to methylphenidate, a common ADHD medication [14, 22, 28–30]. The variants decrease expression or function of LPHN3 protein. *LPHN3* has also been associated with substance abuse disorders, which can be comorbid with ADHD [31, 32].

We developed an *Lphn3* knock-out (KO) rat. These rats are hyperactive in both novel and familiar environments. They under-respond to amphetamine, have increased levels of striatal tyrosine hydroxylase (TH), amino acid decarboxylase (AADC), and dopamine (DA) transporter (DAT) and decreased levels of DA D1 receptor (DRD1) and DARPP-32 in striatum with no changes in in LPHN1, LPHN2, or FLRT3 [33]. The KO rats also exhibit increased spontaneous striatal DA release by fast scan cyclic voltammetry [34]. Here we show that LPHN3 deletion has selective effects on some types of L&M while sparing others.

Materials and Methods

Sprague Dawley rats heterozygous for *Lphn3* were bred in-house and maintained in polysulfone cages in a pathogen free vivarium using Modular Caging with woodchip bedding and steel enclosures for enrichment [35] with HEPA filtered air (30 air changes/h; Alternative Design, Siloam Spring, AR). Water was reverse-osmosis/UV light sterilized and food was autoclaved NIH-07 diet (LabDiet, Richmond, IN). Rats were maintained on

a 14 h light, 10 h dark cycle (lights on at 600 h). The protocol was approved by the Cincinnati Children's IACUC. The vivarium is accredited by AAALAC International. At weaning (postnatal day [P]28), rats were housed in pairs with littermates by sex. Testing was conducted by personnel blind to genotype. The number of rats used for each genotype is provided in figure captions.

Of the three known members of the LPHN3 sub-family, LPHN3 was targeted because of its association with ADHD and expression in brain regions associated with L&M. The sub-family is alternatively named adhesion G protein-coupled receptor L (ADGRL1-3) [OMIM 616417]. The CRISPR/Cas9 targeting of exon-3 is as described [36]. *Lphn3*$^{+/-}$ males and females were bred to generate offspring for testing. Ear clips from offspring were collected on P7 for PCR genotyping [36]. If a litter had more than one offspring/sex/genotype, a random number table was used to select one male and one female KO and WT rat for each experiment to control for litter effects [37, 38]. Based on prior data with the *Lphn3* KO rats [33] we estimated a sample size of 20 per group per sex was needed therefore, we enrolled 20 litters using only those litters that had all genotypes by sex required. On P7, litters were genotyped and 2 male and 2 female KO and 2 male and 2 female WT rats were retained but only 1 of each per genotype/sex was tested; all litters were culled to 8 (4 males and 4 females).

Experiment-1

Learning tests were chosen that are associated with different brain regions. For egocentric/striatal dependent navigation we used the Cincinnati water maze (CWM) test, conducted in the dark to prevent use of distal cues [39]. For spatial/hippocampal dependent L&M we used the Morris water maze (MWM) with reversal and shift phases for cognitive flexibility. For amygdala-related memory we used conditioned freezing and for recognition memory novel object recognition (NOR).

Straight Channel.

Before CWM testing, rats received training in a straight channel to acclimate them to swimming, the submerged escape platform, and to measure swim speed. Rats received 4 trials in a 244 cm long × 15 cm wide × 50 cm high channel filled halfway with water with a submerged escape platform at one end. Latency to reach the platform was recorded.

Cincinnati Water Maze.

This is an egocentric navigation test [39] that consists of 10 T-shaped cul-de-sacs branching from a central path that extends from the start to the goal (Fig. 1B). The maze is 51 cm deep filled hallway with water (21 ± 1 °C). To prevent use of distal cues, only infrared light was provided. An infrared sensitive camera was mounted above the maze connected to a monitor in an adjacent room where the experimenter recorded errors and latency. An error was counted when the head and forelimbs entered into the stem of any dead-end cul-de-sac or into the crossing-arm of a "T". Rats were given 2 trials/day with a 5 min limit/trial for 18 days and a 5 min intertrial interval if they failed to find the platform on the first trial of the day.

Morris Water Maze.

Rats were tested in the MWM to assess spatial learning and reference memory [40]. The maze was a 244 cm diameter × 51 cm high circular pool made of black polypropylene filled halfway with water (21 ± 1 °C). The room had prominent distal cues (geometric designs and posters on the walls). Testing consisted of: (1) acquisition, (2) reversal, (3) shift, and (4) cued-random phases. The first three phases consisted of 4 trials/day (2 min limit/trial) for 6 days to find the hidden platform from pseudo-random start locations followed on day-7 by a 45 s probe trial with no platform and average distance from the platform was calculated. For acquisition, a 10 cm diameter platform in the SW quadrant was used [40]. For reversal, a 7 cm diameter platform in the NE quadrant was used. For shift, a 5 cm diameter platform in the NW quadrant was used. A camera above the maze tracked performance using AnyMaze video tracking (Stoelting Co., Wood Dale, IL). For the learning trials, path efficiency was calculated as a straight line from the start to the platform divided by the path the rat took to reach the platform. The fourth phase was cued-random. Curtains were closed around the pool to block distal cues. A plastic ball was mounted on a steel rod 10 cm above the water on a 10 cm diameter platform. Rats were given 4 trials/day for 2 days with both the platform and start positions pseudo-randomly changed on every trial and latency recorded.

Conditioned Freezing.

On day-1, rats were placed in 25 cm × 25 cm acrylic test boxes with metal grid floors (San Diego Instruments, San Diego, CA). The chambers were placed in sound-attenuating cabinets. Day-1 consisted of 6 min acclimation, followed by 6 min of alternating 82 dB tones for 30 s with a 1 s, 0.9 mA foot-shock at the end of tone presentation. Tone-shock pairings were repeated 3 times 180 s apart. On day-2, rats were placed back in the test chamber for 6 min (no tone or shock). On day 3, rats were placed in a different chamber (triangular with a solid floor, half the size of the original chamber) for 6 min with no tone or shock, followed by 6 min with tone present. Movement was detected by photobeam interruptions.

Long-Term Potentiation (LTP).

P35 rats were used for LTP (6 litters: 1 male/genotype/litter). Brains were removed and placed in cold artificial cerebral spinal fluid (aCSF: 124 mM NaCl, 3 mM KCl, 1.25 mM NaH_2PO_4/H_2O, 1 mM $MgCl_2/6H_2O$, 10 mM glucose, 2 mM $CaCl_2$, 26 mM $NaHCO_3$) saturated with 95% O_2/5% CO_2 and chilled for 1–2 min, and mounted on a vibratome (Vibratome 1500, Warner Instruments, Hamden, CT). Parasagittal sections (350 μm) were cut and maintained in a bath of oxygenated aCSF at 32 °C for ~1 h. LTP was conducted using a MED64 multielectrode system (Alpha Med Sciences, Kadoma, Japan). Electrodes were 50 μm × 50 μm, spaced 150 μm apart [41]. Pulses were delivered to CA1, and fEPSPs were recorded from distal electrodes until a 10 min stable baseline was obtained. Then a theta burst [tetanus = 100 Hz in 10 bursts (4 pulses/burst) delivered at 5 Hz for 2 s] was applied and fEPSPs and slope recorded for 90 min.

Western blotting.

Western blots were done on 8 WT and 8 KO female rats. Frozen tissue was homogenized in radioimmuno-precipitation buffer (25 mM Tris, 150 mM NaCl, 0.5% sodium deoxychlorate, and 1% Triton X-100) adjusted to 7.2 pH with protease inhibitor (Pierce Biotechnology, Rockford, IL). Protein samples were diluted to 3 μg/μL and quantified using the BCA™ Protein Assay Kit (Pierce Biotechnology, Rockford, IL). Western blots were performed using LI-COR Odyssey® (LI-COR Biosciences, Lincoln, NE). Samples (25 μL) were mixed with Laemmli buffer (Sigma, USA) and loaded on 12% gel (Bio-Rad Laboratories, Hercules, CA) and run at 200 V for 35 min in running buffer (25 mM Tris, 192 mM glycine, 0.1% SDS). Gels were transferred to Immobilon-FL transfer membrane (Millipore, USA) in 1X rapid transfer buffer (AMRESCO, Solon, OH) at 40 V for 1.5 h and membranes were soaked in Odyssey phosphate buffered saline blocking buffer for 1 h, then incubated overnight at 4 °C with primary antibody in blocking buffer with 0.2% Tween 20. Membranes were incubated with secondary antibody in blocking buffer 0.2% Tween 20 and 0.01% SDS for 1 h at room temperature. Antibodies were as follows: rabbit anti-NMDA-NR1 (Ab109182, AbCam, Cambridge, MA) at 1:4000 with Odyssey IRDye 800 secondary antibody at 1:3,000 dilution; rabbit anti-NMDA-NR2A (Ab124913, AbCam, Cambridge, MA) at 1:9,000 with Odyssey IRDye 800 secondary antibody at 1:20,000 dilution; rabbit anti-NMDA-NR2B (Ab81271, AbCam, Cambridge, MA) at 1:5,000 with Odyssey IRDye 800 secondary antibody at 1:20,000 dilution. Relative protein levels were quantified using the LI-COR Odyssey® scanner and Image Studio software.

Experiment-2

Because the KO rats had impaired learning in the MWM that depends on distal cues and on cued trials, the question arose of whether the KO rats had visual impairment. There is evidence that *Lphn3* is expressed in the visual system [42]. Prepulse inhibition (PPI) of acoustic startle assesses sensorimotor gating using a weaker prepulse or a prepulse of a different modality to inhibit the response. We used a light prepulse to determine if visual detection was present.

Light Prepulse Inhibition of Acoustic Startle.

A group of 20 naïve rats (5/sex/genotype) from 10 new litters were tested for PPI of acoustic startle with light prepulse in SR-LAB startle chambers (San Diego Instruments, San Diego, CA). Rats were placed in cylindrical holders mounted on a platform with piezoelectric accelerometers attached to the underside that detect movement. Background noise was 55 dB. The acoustic pulse was a 120 dB SPL white noise burst, 1.5 ms rise time. The light prepulse was generated by a panel of LEDs (~1100 lux) that does not elicit a startle response itself [43]. Each rat received trials at prepulse-pulse intervals of 30, 70, or 100 ms before the pulse. Stimulus duration was 20 ms. Trials were presented in a Latin square sequence repeated to generate 20 trials of each type. Responses were recorded for 100 ms after pulse onset. The dependent measure was maximum startle amplitude measured in mV (V_{max}).

Experiment-3

In experiment-1 KO rats had deficits on egocentric and spatial L&M but not on conditioned freezing for context or cue, yet KO rats did detect light prepulses. It may be that KO rats can learn the mazes but at a slower rate than WT rats. This experiment used 20 rats in two cohorts of 5 male WT and 5 male KO littermate pairs. As before, rats received straight swim channel training. On the first day of MWM, rats were given extra training to reduce or eliminate performance factors unrelated to spatial learning [44, 45]. Subsequently, rats received MWM hidden platform trials (4 trials/day). The number of test days was extended for KO rats. WT rats were not tested after they reached asymptotic performance (day-6) whereas KO rats continued for another 6 days.

To assess the ability of KO rats to use visual stimuli in other ways we assessed NOR and temporal order (associated with hippocampus and perirhinal cortex) [46, 47] and conditioned freezing with a protocol that increased the conditioning prior to memory trials. After testing, brains were examined by immunohistochemistry.

Straight Channel.

Same as above.

Morris Water Maze.

Prior to hidden platform trials, rats were first given one day of training in the maze to a visible cue to ensure learning of the subordinate non-spatial aspects of the task. Rats were assessed as above except that they were also given a training phase in the MWM and 12, rather than 6 days, of hidden platform acquisition trials. For training, curtains were closed around the maze to block distal cues. Rats received 6 trials using a fixed start and platform position. The platform was 10 cm diameter, submerged with an orange ball mounted to a pole 10 cm above the water. The day after training, rats were given four trials per day for 12 days to find a hidden 10 cm diameter platform in the SW quadrant with curtains open to expose distal cues. Rats were started from 4 different locations around the perimeter on each trial. When WT rats reached asymptotic performance, they were discontinued from testing. KO rats continued testing until they reached WT performance levels or up to a limit of 12 days. Time limit/trial was 90 s. Rats not finding the platform were placed directly on it for 5–10 s before being returned to their cage. Rats were tested in small groups. In each test group (balanced for genotype), all rats received trial-1 in turn before the sequence started over for trial-2, etc. All other procedures were as before.

Novel Object Recognition.

On day 1, each rat was placed in a 40 × 40 cm test arena with four different objects, one in each corner of a black acrylic AnyBox (Stoelting) with AnyMaze video tracking. Rats were habituated to 4 objects for 10 min. Day-2 was familiarization for 10 min with 4 objects different from those used on Day-1. Novel preference was tested 1 h later by placing the rat back in the chamber with 3 copies of the familiarization objects and one new object. Rats remained in the chamber until they accumulated 30 s of object exploration [48] up to a limit of 10 min.

Temporal Order.

Rats were tested in AnyBox a week after NOR. For step-1 each rat was placed in the test arena with two identical objects in opposite corners until it reached 30 s object exploration. For step-2, 4 h later, rats were placed in the chamber with two new objects until they reached 30 s of exploration time. Preference was tested 1 h later by placing each rat in the chamber with 1 of each of the previous objects until they reached the 30 s exploration criterion.

Conditioned Freezing.

This was the same as before with the following changes: Day-1 was 6 min of acclimation followed by 6 min of conditioning with compound cues of an LED light (2 kHz) and tone (85 dB) for 30 s paired with a 1.3 mA foot-shock during the last 2 s of the light-tone interval. The light-tone-shock pairing was repeated 9 times at 30 s intervals. On day-2, rats were placed in the same box for 6 min with no tone/light or foot-shock. On day-3, rats were placed in a different hexagonal box with approximately the same floor area as that used on day-1 for 6 min. For the first 3 min no tone was presented then each rat received 10 trials of 30 s light-tone-on and 30 s with no stimuli.

Immunohistochemistry: Nissl histology.—Nissl staining was conducted on 5 male WT and KO rats from 5 different litters. Rats were anesthetized with pentobarbital and perfused with 4% PFA solution (pH 7.4). Brains were removed and stored in 4% PFA. The following day, brains were transferred to 30% sucrose in 1 X PBS solution. After brains sank, coronal sections (40 μm) were cut on a cryostat and mounted on slides and left overnight. Slides were then immersed in xylene and rehydrated in alcohol for 5 min per concentration (100%, 95%, 70%). Slides were then dipped in ddH_2O, and then transferred to a 0.5% cresyl violet stain for 30 min. Slides were then dehydrated in alcohol for 5 min a piece (70%, 95%, 100%) before mounting with Permount. After mounting medium had hardened, sections were imaged using a Nikon NiE upright Widefield at 4 X magnification under bright field illumination.

Experimental Design and Statistical Analysis

All experiments were factorial designs. Experiment-1 had 20 liters and was a 2-between (genotype and sex) by 1-random (litter) factor or a 2-between by 1-within (trial or day) by 1-random (litter) factorial ANOVA [49, 50]. Data were analyzed using mixed linear model ANOVAs (Proc Mixed, SAS v9.4, SAS Institute, Cary, NC) with restricted maximum likelihood estimation. Only one rat/genotype/sex/litter was used. Experiment-2 used 5 litters and Experiment-3 20 litters. Covariance models of best fit were evaluated using the AICC test. The best fit models were autoregressive (AR) or AR moving average (ARMA). Kenward-Roger first order degrees of freedom were used with Type III ANOVAs. Significant interactions with a repeated measure factor were analyzed using slice-effect ANOVAs from the Mixed models. Western blot data were analyzed by t-test for independent samples following a Folded F test for homogeneity of variance. Statistical tests were two-sided with significance set at $p < 0.05$. Data are presented as least square mean ± SEM.

Results

Experiment-1

Straight channel training—Training trials acclimate rats to swimming and platform escape [39]. There were effects of genotype [$F(1,86.6) = 32.17$, $p < 0.0001$] and genotype × trial [$F(3,208) = 3.4$, $p < 0.05$]. On the first two trials, KO rats had longer latencies than WT rats (Fig. 1A) but not on trials 3 and 4. There was no effect of sex or interaction of sex × genotype.

Egocentric learning (Cincinnati water maze)—The maze is illustrated in Fig. 1B. There was an effect of genotype on errors [$F(1,172) = 68.35$, $p < 0.0001$] and a genotype × day interaction [$F(17,1201) = 2.65$, $p < 0.0003$], Fig. 1C. Similarly, there was an effect of genotype on escape latency [$F(1,124) = 44.64$, $p < 0.0001$] and a genotype × day interaction [$F(17,1250) = 2.93$, $p < 0.0001$], Fig. 1D. KO rats had longer latencies and increased errors compared with WT rats starting on day-7 and did not catch up to WT levels throughout the test, but they did improve over days. There were no main effects or interactions with sex.

Spatial Learning and Memory (Morris water maze)—Day-1 data were analyzed by trial to determine if KO rats started equally with WT rats. For path efficiency, the main effect of genotype was significant [$F(1,112) = 12.98$, $p < 0.0005$] as was the genotype × trial interaction [$F(3,205) = 4.63$, $p < 0.005$], Fig. 2A. KO did not differ from WT on trial-1, had reduced path efficiency on trials 2–4. There was no significant main effect of sex or interactions with sex.

Analysis of all days of acquisition for path efficiency showed effects of genotype [$F(1,103) = 103.35$, $p < 0.0001$] and genotype × day [$F(5,346) = 5.53$, $p < 0.0001$], Fig. 2B. The KO rats had reduced path efficiency compared with WT rats on all days. The same pattern was found for latency: genotype [$F(1,95.3) = 159.60$, $p < 0.0001$] and genotype × day [$F(5,347) = 3.18$, $p < 0.01$] (not shown). On the probe trial 24 h after the last acquisition trial, KO rats had increased average distance to the former platform site compared with WT rats [$F(1,54.2) = 45.47$, $p < 0.0001$], Fig. 2C.

After acquisition, the platform was moved to the opposite quadrant and rats were tested in reversal for cognitive flexibility. For path efficiency on the first day analyzed by trial, KO rats started out comparable with WT rats on trial-1 and diverged on trials 2–4. The main effect of genotype was significant [$F(1,91.5) = 21.37$, $p < 0.001$] as was the genotype × trial interaction [$F(3,202) = 6.03$, $p < 0.0006$], Fig. 2D. There were no sex-related effects. When data for all days were analyzed, for path efficiency there was an effect of genotype [$F(1,95.1) = 1463.18$, $p < 0.001$], Fig. 2E, and for latency [$F(1,95.1) = 143.18$, $p < 0.0001$] (data not shown), and no interactions. The KO rats had reduced path efficiency and longer latencies compared with the WT rats. There were no sex-related effects. On the reversal probe trial, KO rats had increased average distance to the former platform site compared with WT rats [$F(1,57.4) = 32.0$, $p < 0.001$], Fig. 2F. The main effect of sex was not significant nor were there any interactions with sex.

The day after reversal, the platform was moved (shifted) a second time to an adjacent quadrant. On the first day of shift analyzed by trial for path efficiency, there was a main effect of genotype [(1,107) = 44.27, p<0.0001)]. There was also a genotype × trial interaction [F(3,228) = 10.01, p< 0.0001], Fig. 2G. There were no differences on trial-1 but on trials 2–4, KO rats were significantly less efficient than WT rats. There were no sex-related effects. When data for all days were analyzed, there was an effect of genotype on path efficiency [F(1,97.1) = 128.76, p< 0.0001] and a genotype × day interaction [(5,345) = 3.37, p<0.01] Fig. 2H; latency was similarly affected [F(1,75.9) = 128.08, p< 0.0001] except that for this outcome there was a genotype × sex interaction on latency [F(1,72.1) = 5.62, p<0.02] not seen on path efficiency or path length. This was attributable to female KO rats having longer latencies than male KO rats compared with WT counterparts. On the shift probe trial, KO rats had increased average distance to the former platform site compared with WT rats [F(1,52.5) = 41.9, p< 0.001], Fig. 2I. Despite the large deficits in KO rats, they showed some learning on all phases.

After shift, rats were given cued-random trials with curtains closed around the maze with start and platform positions moved on every trial. There was an effect on latency of genotype [F(1,70) = 29.15, p< 0.0001] and genotype × day [(F(1,66.4) = 4.38, p<0.05]. Slice-effect ANOVAs showed an effect on day-1 [F(1,82.3) = 21.1, p< 0.0001]. As can be seen in Fig. 3A, both groups improved from trial-1 to trial-2, but KO rats had longer latencies on all trials. On day-2, there was also a genotype effect [F(1,80.5) = 37.7, p< 0.001] and a genotype × trial interaction [F(3,204) = 3.3, p< 0.02]. For the interaction, slice analyses showed that KO rats took longer than WT rats on all trials, Fig. 3B.

Conditioned Freezing—On day-1, KO rats were not hyperactive as expected but had slightly reduced exploration habituation compared with WT rats [F(1,110) = 3.9, p< 0.05], Fig. 3C (pre-stimulus). During conditioning, KO rats became more active than WT rats [F(1,110) = 11.1, p< 0.001], Fig. 3C. On day-2 (contextual memory) and day-3 (cued memory) no effects of genotype were seen (Fig. 3D, E).

Long-term Potentiation—As shown in Fig. 4, KO rats had reduced early LTP compared with WT rats [F(1,47.6) = 5.76, p< 0.05], whereas late LTP was not affected that resulted in a genotype × interval interaction [F(269,2515) = 1.34, p< 0.001].

NMDA receptors—NMDA-NR1 levels were decreased in the hippocampus of KO rats compared with WT rats [t(10) = −3.23, p < 0.01], Fig 5A,B. No differences were seen in NR2A [(t(10) = −0.14, p = 0.8898)], Fig. 5C,D, or NR2B [(t(10) = −0.56, p = 0.66)], Fig. 5E,F.

Experiment-2

Flash Prepulse Inhibition of Startle—KO rats had normal contextual and cued freezing suggesting that they are not visually impaired, but because they performed poorly in the MWM cued-random test, we tested visual detection using light PPI. For light PPI of acoustic startle, there was a nearly significant effect of genotype (F(1,16.6) = 4.23, p = 0.055) and an effect of prepulse interval (F(4,59.8) = 9.22, p < 0.0001), Fig. 5G for the maximum

response (V_{max}). While KO rats had increased startle amplitude, the light prepulse inhibited the response at the 30, 70, and 100 ms delays but not at 400 ms, regardless of sex.

Experiment-3

Straight Channel—There was no effect of genotype or trial, and no interaction of genotype × trial Fig. 6A.

Morris Water Maze—During training, on day-1, there was a main effect of genotype [$F(1,27.1) = 26.26$, $p < 0.0001$] and trial [$(5,79) = 6.25$, $p<0.0001$) but no genotype × trial interaction (Fig. 6B). On day 2, there was also a main effect of genotype [$F(1,21.5) = 108.45$, $p < 0.0001$] and a trend for an effect of trial ($p<0.077$). On both days, KO rats had longer latencies compared with WT rats.

During acquisition, KO rats had increased latency compared with WT rats on days 1–6 [$F(1, 18.5) = 42.08$, $p < 0.0001$] Fig. 6D (left). There was a main effect of day [$F(5, 64.6) = 5.34$, $p < 0.001$]. There was no genotype × day interaction. For path efficiency, the pattern was similar in which KO rats had decreased path efficiency compared with WT rats on days 1–6 [$F(1, 9.06) = 27.84$, $p < 0.0001$] and there was a genotype × day interaction [$F(5, 65.3) = 4.96$, $p < 0.0001$] Fig 6E (days 1–6). Differences between groups remained on extra test days (7–12) done to determine if KO rats could eventually catch up. Because WT rats were not tested on days 7–12 there was no to which KO performance could be compared statistically, nevertheless the group differences on latency were clear, Fig. 6D (days 7–12). The same pattern was seen for path efficiency on days 7–12, Fig. 6E (days 7–12). Despite extra training and the extra acquisition trials, KO rats reached asymptotic performance at levels far worse than those of WT rats. Heat maps of the WT rats and of the KO rats subdivided into those that learned (albeit poorly) and those that never learned are shown in Fig. S1 for each day of acquisition. WT rats are shown in the left column, KO learners in the middle column, and KO non-learners in the right column. Density of time spent in an area starts as blue and changes to green as overlap in swim pattern increases. Even on day-1, KO non-learners had high density around the perimeter with no patterns away from the wall. This pattern never changed for these rats from day-1 through day-6. By contrast, WT rats searched in the periphery on day-1 and 2 but then their pattern shows a halo around the platform with high density directly on the platform zone. KO learners on day-1 were predominantly peripheral searching, but this changed on day-2, and changes further on day-3, 4, and 5, with clustering in the target quadrant by day-6, but still more scattered than for WT rats. Tracings of representative rats on the probe acquisition trial are shown in Fig. S2. Panels A and B show the path of two WT rats in reaching the location where the platform used to be. As can be seen the path is direct and precise. Panels C and D show the pattern of two KO learners who could find the platform on 2 min acquisition trials, but on 45 s probe trials only started to venture away from the wall (panel D) or had not yet ventured away from the wall. Panel E and F show two non-learners that stayed close to the wall for the entire 45 s probe trial. These patterns reveal that KO rats are not only spatially impaired, but some are more severely affected than others. The basis for the individual differences is not yet known.

Novel Object Recognition and Temporal Order—For NOR there were no genotype effects on familiarization or retention. Both groups performed similarly on retention showing similar preference for the novel object, Fig 7A. There were no differences in time to reach criterion. For temporal order, there were no genotype effects on percent time spent with object 1. Both groups showed little preference for object 1 during retention, Fig 7B.

Nissl Staining—There were no observable morphological differences between *Lphn3* KO and WT rats in the hippocampus (Fig 8A,B) or in any other region (Fig. 8C,D).

Discussion

LPHN3 is involved in synaptic function in the CA1 region [51], suggesting a role in neuroplasticity. *Lphn3* deletion in mice, zebrafish, *Drosophila*, and rats results in hyperactivity [33, 52–55] and in people variant expression of the gene is associated with ADHD [27, 56, 57]. However, the role of LPHN3 in cognitive function is unknown. ADHD patients sometimes exhibit cognitive deficits, suggesting overlapping neural circuitry [58–60]. When *Lphn3* is deleted, it results in effects on egocentric and allocentric L&M, LTP, and NMDA receptor levels while sparing conditioned freezing and object recognition, demonstrating that the effects are selective. However, on those forms of L&M that were affected, the effects are large which indicates that LPHN3 is critical for these functions. The learning and memory deficits in the KO rats may recapitulate aspects of the cognitive endophenotype seen in some ADHD patients. ADHD is polygenic with multiple small-effect variants. *LPHN3* is only one such variant, and the *Lphn3* KO rat is a gene deletion model. Therefore, while the KO rat can help elucidate the function of this protein it does not address the way variants in this gene in humans interacts with gene variants that lead to ADHD. Creating point mutations in animals of the 21 variants found in humans with *LPHN3*-associated ADHD would be challenging but would likely be informative. As CRISPR/Cas9 methods advance creating more nuanced models of *LPHN3* variants should become more accessible. *LPHN3* variants are also implicated in substance use disorders [31, 32]. We have yet to explore conditioned place preference or other models relevant to substance use disorders with the current KO model but plan to do so.

It is known that egocentric/procedural L&M depends on striatal DA, including learning the path to escape in the CWM where no distal cues are present [39, 61, 62], and on the lateral entorhinal cortex [63]. *Lphn3* KO rats have decreased neostriatal DRD1 and DARPP-32 levels, accompanied by increased DAT and TH levels [33]. These data are consistent with egocentric L&M deficits being associated with dysregulated DA in the striatum. ADHD is thought to be the result of DA hypofunction with compensatory increases in DA release [64]. Variations in DAT [65] and DA receptors [66, 67] are implicated in ADHD to which *LPHN3* variants are now included. Given that ADHD is polygenic with multiple small effect gene contributions and probable environmental factors, the observation that LPHN3 variants occur in only some ADHD patients is not surprising [68]. Our *Lphn3* KO rat is a null mutation rather than an under-expressed variant as in humans, nevertheless the phenotype in the KO rats is consistent with the hyperactivity and cognitive changes seen in ADHD but the phenotype is more severe in KO rats. In addition, those with ADHD *LPHN3* variants show better responsiveness to psychostimulants and these drugs all act primarily on DA

signaling [14]. Interspecies similarities include the rescue of hyperactivity in *lphn3.1* KO zebrafish with drugs known to reduce ADHD symptoms [52, 53] and reduced locomotor activity after amphetamine relative to baseline in KO rats [36]. This is not to suggest that only the striatum is involved in the effects seen in *Lphn3* KO rats, but rather that the striatum plays an important role in egocentric navigation.

The KO rats also exhibit spatial deficits and reference memory impairments in the MWM. In addition, KO rats have impaired cognitive flexibility as reflected in reversal and shift phase deficits. This likely reflects involvement of LPHN3 in networks extending beyond the hippocampus and entorhinal cortex known to be involved in spatial memory and alterations in glutamatergic function. MWM allocentric deficits are consistently associated with hippocampal dysfunction [2, 17, 18, 69], whereas MWM cued deficits are more often associated with egocentric deficit, however cued trials in the MWM are not as demanding as path finding in the CWM. Consistent with glutamatergic mediated spatial deficits, LTP during the first post-tetanus hour in CA1 was blunted in KO rats, and NMDA-NR1 subunits were downregulated. Impaired early LTP in CA1 is often seen in conjunction with reduced NMDARs along with spatial L&M impairment [70–72], albeit with exceptions [73]. The fact that LPHN3 impairs navigational learning in the same brain regions where LPHN3 is abundantly expressed (striatum and hippocampus) is noteworthy [11, 33]. Further studies should investigate the circuits involved in egocentric and allocentric L&M and their interconnections.

Performance in the MWM requires visual use of distal cues which triggered questions about sight in the KO rats, but several tests revealed that they can use visual cues to suppress startle responses, recognize unfamiliar from familiar objects, and respond equally to contextual cues as WT rats. Hence, the data are inconsistent with visual impairment.

In sum, *Lphn3* KO rats have pronounced, but selective, L&M deficits. They are impaired in striatally mediated egocentric/procedural and hippocampally mediated spatial navigation without impairment of conditioned contextual or cued memory or on recognition memory. Hence, LPHN3 plays a role in cognitive function as well as hyperactivity and may have implications as a therapeutic target for ADHD since a high percentage of small molecule therapeutic drugs target GPCRs.

Supplementary Material

Refer to Web version on PubMed Central for supplementary material.

Funding:

This research was supported by NIH T32 ES007051 (E.M.P.), a grant from the L.I.F.E Foundation, NIH R21 MH110609, and the University of Cincinnati Graduate School Dean’s Dissertation Completion Fellowship (S.L.R). Behavioral testing was conducted through the Animal Behavior Core of Cincinnati Children’s Research Foundation.

References

1. Silva JP, et al., Latrophilin 1 and its endogenous ligand Lasso/teneurin-2 form a high-affinity transsynaptic receptor pair with signaling capabilities. Proc Natl Acad Sci U S A, 2011. 108(29): p. 12113–8. [PubMed: 21724987]
2. O'Sullivan ML, et al., FLRT proteins are endogenous latrophilin ligands and regulate excitatory synapse development. Neuron, 2012. 73(5): p. 903–10. [PubMed: 22405201]
3. Boucard AA, Ko J, and Sudhof TC, High affinity neurexin binding to cell adhesion G-protein-coupled receptor CIRL1/latrophilin-1 produces an intercellular adhesion complex. J Biol Chem, 2012. 287(12): p. 9399–413. [PubMed: 22262843]
4. Lu YC, et al., Structural Basis of Latrophilin-FLRT-UNC5 Interaction in Cell Adhesion. Structure, 2015. 23(9): p. 1678–1691. [PubMed: 26235030]
5. Rahman MA, et al., Norepinephrine exocytosis stimulated by alpha-latrotoxin requires both external and stored Ca2+ and is mediated by latrophilin, G proteins and phospholipase C. Philos Trans R Soc Lond B Biol Sci, 1999. 354(1381): p. 379–86. [PubMed: 10212487]
6. Sudhof TC, alpha-Latrotoxin and its receptors: neurexins and CIRL/latrophilins. Annu Rev Neurosci, 2001. 24: p. 933–62. [PubMed: 11520923]
7. Kreienkamp HJ, et al., The calcium-independent receptor for alpha-latrotoxin from human and rodent brains interacts with members of the ProSAP/SSTRIP/Shank family of multidomain proteins. J Biol Chem, 2000. 275(42): p. 32387–90. [PubMed: 10964907]
8. Krasnoperov VG, et al., alpha-Latrotoxin stimulates exocytosis by the interaction with a neuronal G-protein-coupled receptor. Neuron, 1997. 18(6): p. 925–37. [PubMed: 9208860]
9. Longenecker HE Jr., et al., Effects of black widow spider venom on the frog neuromuscular junction. Effects on end-plate potential, miniature end-plate potential and nerve terminal spike. Nature, 1970. 225(5234): p. 701–3. [PubMed: 4312878]
10. Clark AW, et al., Effects of black widow spider venom on the frog neuromuscular junction. Effects on the fine structure of the frog neuromuscular junction. Nature, 1970. 225(5234): p. 703–5. [PubMed: 4312879]
11. Linets'ka MV, Storchak LH, and Himmelreich NH, [Effect of synaptosomal cytosolic [3H]GABA pool depletion on secretory ability of alpha-latrotoxin]. Ukr Biokhim Zh (1999), 2002. 74(3): p. 65–72.
12. Matsushita H, Lelianova VG, and Ushkaryov YA, The latrophilin family: multiply spliced G protein-coupled receptors with differential tissue distribution. FEBS Lett, 1999. 443(3): p. 348–352. [PubMed: 10025961]
13. Ichtchenko K, et al., A novel ubiquitously expressed alpha-latrotoxin receptor is a member of the CIRL family of G-protein-coupled receptors. J Biol Chem, 1999. 274(9): p. 5491–8. [PubMed: 10026162]
14. Arcos-Burgos M, et al., A common variant of the latrophilin 3 gene, LPHN3, confers susceptibility to ADHD and predicts effectiveness of stimulant medication. Mol Psychiatry, 2010. 15(11): p. 1053–66. [PubMed: 20157310]
15. Jackson VA, et al., Super-complexes of adhesion GPCRs and neural guidance receptors. Nat Commun, 2016. 7: p. 11184. [PubMed: 27091502]
16. Kreienkamp HJ, et al., The calcium-independent receptor for alpha-latrotoxin from human and rodent brains interacts with members of the ProSAP/SSTRIP/Shank family of multidomain proteins. J. Biol. Chem, 2000. 275(42): p. 32387–32390. [PubMed: 10964907]
17. O'Sullivan ML, et al., LPHN3, a presynaptic adhesion-GPCR implicated in ADHD, regulates the strength of neocortical layer 2/3 synaptic input to layer 5. Neural Dev, 2014. 9: p. 7. [PubMed: 24739570]
18. Sando R, Jiang X, and Südhof TC, Latrophilin GPCRs direct synapse specificity by coincident binding of FLRTs and teneurins. Science, 2019. 363(6429): p. eaav7969. [PubMed: 30792275]
19. Acosta MT, et al., ADGRL3 (LPHN3) variants are associated with a refined phenotype of ADHD in the MTA study. Mol Genet Genomic Med, 2016. 4(5): p. 540–7. [PubMed: 27652281]

20. Bonvicini C, Faraone SV, and Scassellati C, Common and specific genes and peripheral biomarkers in children and adults with attention-deficit/hyperactivity disorder. World J Biol Psychiatry, 2018. 19(2): p. 80–100. [PubMed: 28097908]
21. Ribasés M, et al., Contribution of LPHN3 to the genetic susceptibility to ADHD in adulthood: a replication study. Genes Brain Behav, 2011. 10(2): p. 149–57. [PubMed: 21040458]
22. Hwang IW, et al., Association of LPHN3 rs6551665 A/G polymorphism with attention deficit and hyperactivity disorder in Korean children. Gene, 2015. 566(1): p. 68–73. [PubMed: 25871512]
23. Puentes-Rozo PJ, et al., Genetic Variation Underpinning ADHD Risk in a Caribbean Community. Cells, 2019. 8(8).
24. Franke B, et al., The genetics of attention deficit/hyperactivity disorder in adults, a review. Mol Psychiatry, 2012. 17(10): p. 960–87. [PubMed: 22105624]
25. Domene S, et al., Screening of human LPHN3 for variants with a potential impact on ADHD susceptibility. Am J Med Genet B Neuropsychiatr Genet, 2011. 156b(1): p. 11–8. [PubMed: 21184580]
26. Huang X, et al., LPHN3 gene variations and susceptibility to ADHD in Chinese Han population: a two-stage case-control association study and gene-environment interactions. 2018.
27. Domene S, et al., Screening of human LPHN3 for variants with a potential impact on ADHD susceptibility. Am. J. Med. Genet. B Neuropsychiatr. Genet, 2011. 156B(1): p. 11–18. [PubMed: 21184580]
28. O'Sullivan ML, et al., LPHN3, a presynaptic adhesion-GPCR implicated in ADHD, regulates the strength of neocortical layer 2/3 synaptic input to layer 5. Neural Dev, 2014. 9: p. 7. [PubMed: 24739570]
29. Ranaivoson FM, et al., Structural and Mechanistic Insights into the Latrophilin3-FLRT3 Complex that Mediates Glutamatergic Synapse Development. Structure, 2015. 23(9): p. 1665–77. [PubMed: 26235031]
30. Ribases M, et al., Contribution of LPHN3 to the genetic susceptibility to ADHD in adulthood: a replication study. Genes Brain Behav, 2011. 10(2): p. 149–157. [PubMed: 21040458]
31. Arcos-Burgos M, et al., A common genetic network underlies substance use disorders and disruptive or externalizing disorders. Hum Genet, 2012. 131(6): p. 917–29. [PubMed: 22492058]
32. Arcos-Burgos M, et al., ADGRL3 (LPHN3) variants predict substance use disorder. Translational Psychiatry, 2019. 9(1): p. 42. [PubMed: 30696812]
33. Regan SL, Hufgard JR, Pitzer EM, Sugimoto C, Hu Y-C, Williams MT, Vorhees CV, Knockout of latrophilin-3 in Sprague-Dawley rats causes hyperactivity, hyper-reactivity, under-response to amphetamine, and disrupted dopamine markers. Neurobiology of Disease, 2019. 130: p. 104494. [PubMed: 31176715]
34. Regan SL, et al., Enhanced Transient Striatal Dopamine Release and Reuptake in Lphn3 Knockout Rats. ACS Chem Neurosci, 2020. 11(8): p. 1171–1177. [PubMed: 32203648]
35. Vorhees CV, et al., Effects of neonatal (+)-methamphetamine on path integration and spatial learning in rats: effects of dose and rearing conditions. Int. J. Dev. Neurosci, 2008. 26: p. 599–610. [PubMed: 18502078]
36. Regan SL, et al., Knockout of latrophilin-3 in Sprague-Dawley rats causes hyperactivity, hyper-reactivity, under-response to amphetamine, and disrupted dopamine markers. Neurobiol Dis, 2019. 130: p. 104494. [PubMed: 31176715]
37. Holson RR and Pearce B, Principles and pitfalls in the analysis of prenatal treatment effects in multiparous species. Neurotoxicol. Teratol, 1992. 14: p. 221–228. [PubMed: 1635542]
38. Lazic SE and Essioux L, Improving basic and translational science by accounting for litter-to-litter variation in animal models. BMC. Neurosci, 2013. 14: p. 37. [PubMed: 23522086]
39. Vorhees CV and Williams MT, Cincinnati water maze: A review of the development, methods, and evidence as a test of egocentric learning and memory. Neurotoxicol Teratol, 2016. 57: p. 1–19. [PubMed: 27545092]
40. Vorhees CV and Williams MT, Morris water maze: procedures for assessing spatial and related forms of learning and memory. Nat Protoc, 2006. 1(2): p. 848–58. [PubMed: 17406317]
41. Shimono K, et al., Long-term recording of LTP in cultured hippocampal slices. Neural Plast, 2002. 9(4): p. 249–54. [PubMed: 12959154]

42. Paper W, et al., Elevated amounts of myocilin in the aqueous humor of transgenic mice cause significant changes in ocular gene expression. Exp Eye Res, 2008. 87(3): p. 257–67. [PubMed: 18602390]
43. Regan SL, et al., Effects of Permethrin or Deltamethrin Exposure in Adult Sprague Dawley Rats on Acoustic and Light Prepulse Inhibition of Acoustic or Tactile Startle. 2021.
44. Saucier D and Cain DP, Spatial learning without NMDA receptor-dependent long-term potentiation. Nature, 1995. 378: p. 186–189. [PubMed: 7477321]
45. Bannerman DM, et al., Distinct components of spatial learning revealed by prior training and NMDA receptor blockade. Nature, 1995. 378: p. 182–186. [PubMed: 7477320]
46. Barker GR, et al., Recognition memory for objects, place, and temporal order: a disconnection analysis of the role of the medial prefrontal cortex and perirhinal cortex. J Neurosci, 2007. 27(11): p. 2948–57. [PubMed: 17360918]
47. Barker GR and Warburton EC, When is the hippocampus involved in recognition memory? J Neurosci, 2011. 31(29): p. 10721–31. [PubMed: 21775615]
48. Clark RE, Zola SM, and Squire LR, Impaired recognition memory in rats after damage to the hippocampus. J. Neurosci, 2000. 20(23): p. 8853–8860. [PubMed: 11102494]
49. Golub MS and Sobin CA, Statistical modeling with litter as a random effect in mixed models to manage “intralitter likeness”. Neurotoxicol Teratol, 2020. 77: p. 106841. [PubMed: 31863841]
50. Vorhees CV and Williams MT, Litter effects: Comments on Golub and Sobin’s “Statistical modeling of litter as a random effect in mixed models to manage “intralitter likeness””“. Neurotoxicol Teratol, 2020. 77: p. 106852. [PubMed: 31837394]
51. Sando R, Jiang X, and Sudhof TC, Latrophilin GPCRs direct synapse specificity by coincident binding of FLRTs and teneurins. Science, 2019. 363(6429).
52. Lange M, et al., Pharmacological analysis of zebrafish lphn3.1 morphant larvae suggests that saturated dopaminergic signaling could underlie the ADHD-like locomotor hyperactivity. Prog Neuropsychopharmacol Biol Psychiatry, 2018. 84(Pt A): p. 181–189. [PubMed: 29496512]
53. Lange M, et al., The ADHD-susceptibility gene lphn3.1 modulates dopaminergic neuron formation and locomotor activity during zebrafish development. Mol Psychiatry, 2012. 17(9): p. 946–54. [PubMed: 22508465]
54. Orsini CA, et al., Behavioral and transcriptomic profiling of mice null for Lphn3, a gene implicated in ADHD and addiction. Mol Genet Genomic Med, 2016. 4(3): p. 322–43. [PubMed: 27247960]
55. Wallis D, et al., Initial characterization of mice null for Lphn3, a gene implicated in ADHD and addiction. Brain Res, 2012. 1463: p. 85–92. [PubMed: 22575564]
56. Arcos-Burgos M, et al., A common variant of the latrophilin 3 gene, LPHN3, confers susceptibility to ADHD and predicts effectiveness of stimulant medication. Mol. Psychiatry, 2010. 15(11): p. 1053–1066. [PubMed: 20157310]
57. Arcos-Burgos M and Muenke M, Toward a better understanding of ADHD: LPHN3 gene variants and the susceptibility to develop ADHD. Atten. Defic. Hyperact. Disord, 2010. 2(3): p. 139–147. [PubMed: 21432600]
58. Balint S, et al., Attention deficit hyperactivity disorder (ADHD): gender- and age-related differences in neurocognition. Psychol Med, 2009. 39(8): p. 1337–45. [PubMed: 18713489]
59. Biederman J, et al., Impact of executive function deficits and attention-deficit/hyperactivity disorder (ADHD) on academic outcomes in children. J Consult Clin Psychol, 2004. 72(5): p. 757–66. [PubMed: 15482034]
60. Lambek R, et al., Executive dysfunction in school-age children with ADHD. J Atten Disord, 2011. 15(8): p. 646–55. [PubMed: 20858784]
61. Braun AA, et al., Dopamine depletion in either the dorsomedial or dorsolateral striatum impairs egocentric Cincinnati water maze performance while sparing allocentric Morris water maze learning. Neurobiol Learn Mem, 2015. 118: p. 55–63. [PubMed: 25451306]
62. Braun AA, et al., 6-Hydroxydopamine-Induced Dopamine Reductions in the Nucleus Accumbens, but not the Medial Prefrontal Cortex, Impair Cincinnati Water Maze Egocentric and Morris Water Maze Allocentric Navigation in Male Sprague-Dawley Rats. Neurotox Res, 2016. 30(2): p. 199–212. [PubMed: 27003940]

63. Wang C, et al., Egocentric coding of external items in the lateral entorhinal cortex. Science, 2018. 362(6417): p. 945–949. [PubMed: 30467169]

64. Blum K, et al., Attention-deficit-hyperactivity disorder and reward deficiency syndrome. Neuropsychiatr Dis Treat, 2008. 4(5): p. 893–918. [PubMed: 19183781]

65. Gill M, et al., Confirmation of association between attention deficit hyperactivity disorder and a dopamine transporter polymorphism. Mol Psychiatry, 1997. 2(4): p. 311–3. [PubMed: 9246671]

66. Bobb AJ, et al., Molecular genetic studies of ADHD: 1991 to 2004. Am J Med Genet B Neuropsychiatr Genet, 2005. 132b(1): p. 109–25. [PubMed: 15700344]

67. Swanson JM, et al., Dopamine genes and ADHD. Neurosci Biobehav Rev, 2000. 24(1): p. 21–5. [PubMed: 10654656]

68. Tripp G and Wickens JR, Neurobiology of ADHD. Neuropharmacology, 2009. 57(7–8): p. 579–89. [PubMed: 19627998]

69. Mortimer N, et al., Dissociation of impulsivity and aggression in mice deficient for the ADHD risk gene Adgrl3: Evidence for dopamine transporter dysregulation. Neuropharmacology, 2019.

70. Jedlicka P, et al., A role for the spine apparatus in LTP and spatial learning. Behav Brain Res, 2008. 192(1): p. 12–9. [PubMed: 18395274]

71. Bannerman DM, Rawlins JN, and Good MA, The drugs don't work-or do they? Pharmacological and transgenic studies of the contribution of NMDA and GluR-A-containing AMPA receptors to hippocampal-dependent memory. Psychopharmacology (Berl), 2006. 188(4): p. 552–66. [PubMed: 16676163]

72. Lynch MA, Long-term potentiation and memory. Physiol Rev, 2004. 84(1): p. 87–136. [PubMed: 14715912]

73. O'Mara SM and Aggleton JP, Space and Memory (Far) Beyond the Hippocampus: Many Subcortical Structures Also Support Cognitive Mapping and Mnemonic Processing. Front Neural Circuits, 2019. 13: p. 52. [PubMed: 31447653]

HIGHLIGHTS

- Latrophilin-3 (*Lphn3*) is a synaptic adhesion GCPR involved in regulating signaling
- Variants of *LPHN3* in humans are associated with some cases of ADHD
- *Lphn3* KO rats are hyperactive and release more dopamine shown previously
- Here we show that *Lphn3* KO rats have spatial and egocentric cognitive deficits
- *Lphn3* KO rats also have impaired LTP and reduced NMDA-NR1 in hippocampus

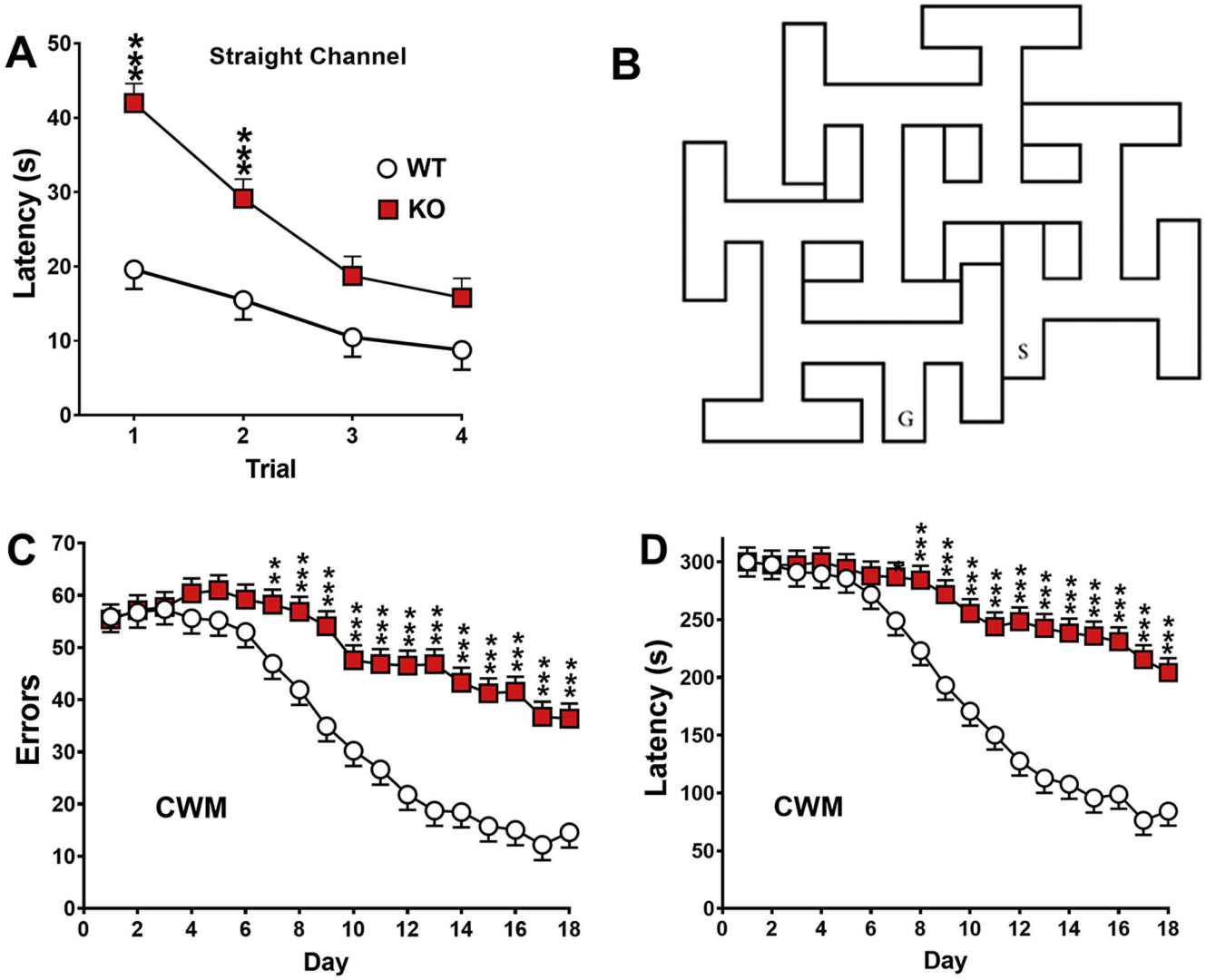

Fig. 1. Experiment-1: Straight Channel and Cincinnati Water Maze (CWM)

A, Latency (Mean ± SEM) to reach the platform during straight channel swimming trials. **B**, Schematic of the CWM, showing start (S) and goal (G) positions. **C**, errors and **D**, latency to escape. Rats were tested for 18 days (2 trials/day). WT n = 39 (♂ 19, ♀ 20); KO n = 40 (♂ 20, ♀ 20). Data are LS Mean ± SE. *p<0.05; **p<0.01, ***p<0.001 compared with WT rats.

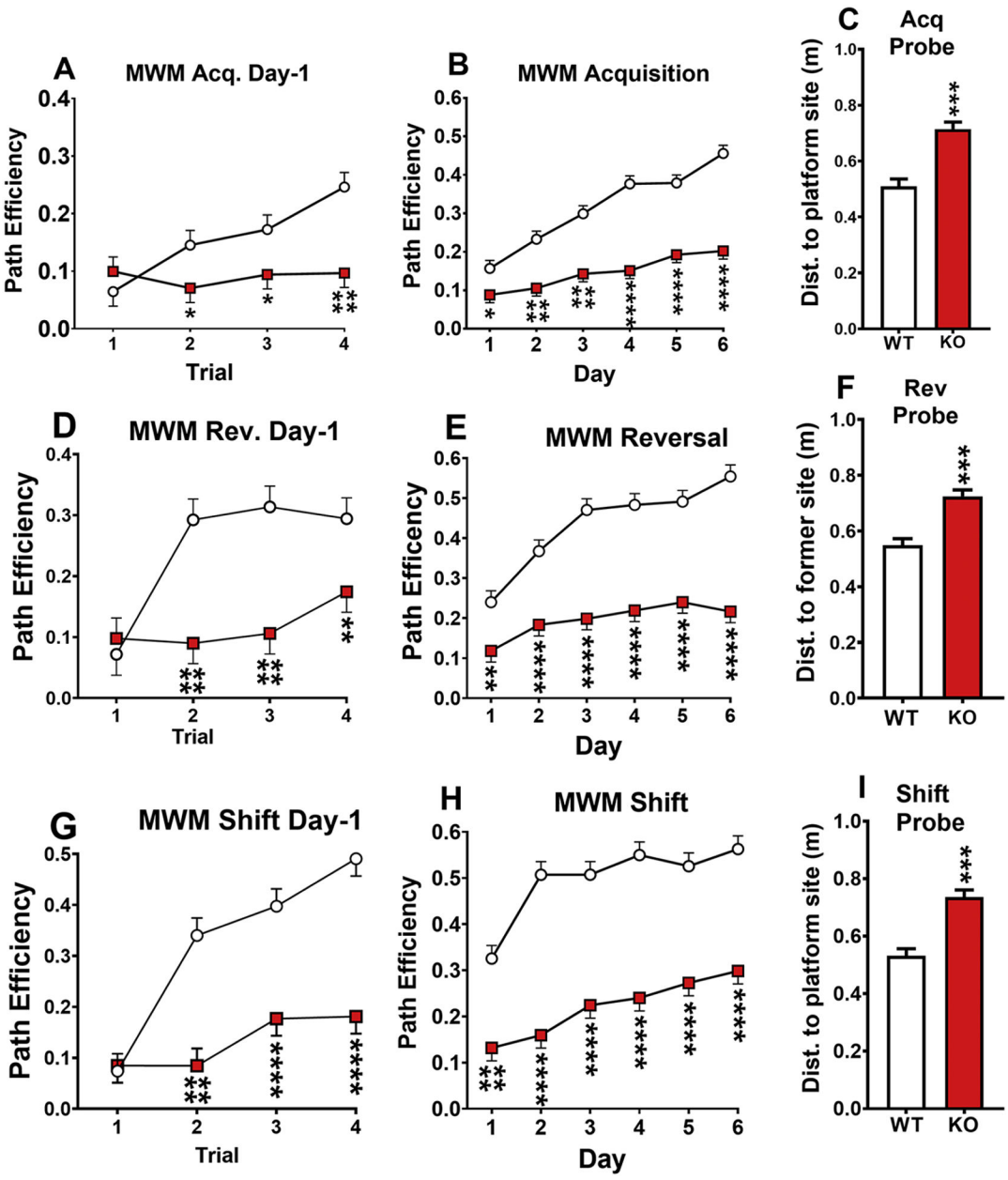

Fig. 2. Experiment-1: Morris Water Maze (MWM)

A, Acquisition path length, day-1 by trial. **B**, Acquisition path length by day. **C**, Acquisition probe trial (average distance to former platform site). **D**, Reversal path length, day-1 by trial. **E**, Reversal path length by day. **F**, Reversal probe trial. **G**, Shift path length, day-1 by trial. **H**, Shift path length by day. **I**, Shift probe trial. In B,E,H rats received 4 trials/day. Path length is in meters. Data are LS Mean ± SEM. WT n = 39 (♂ 19, ♀ 20); KO n = 40 (♂ 20, ♀ 20). ***p<0.001, ****p<0.0001 compared with WT rats.

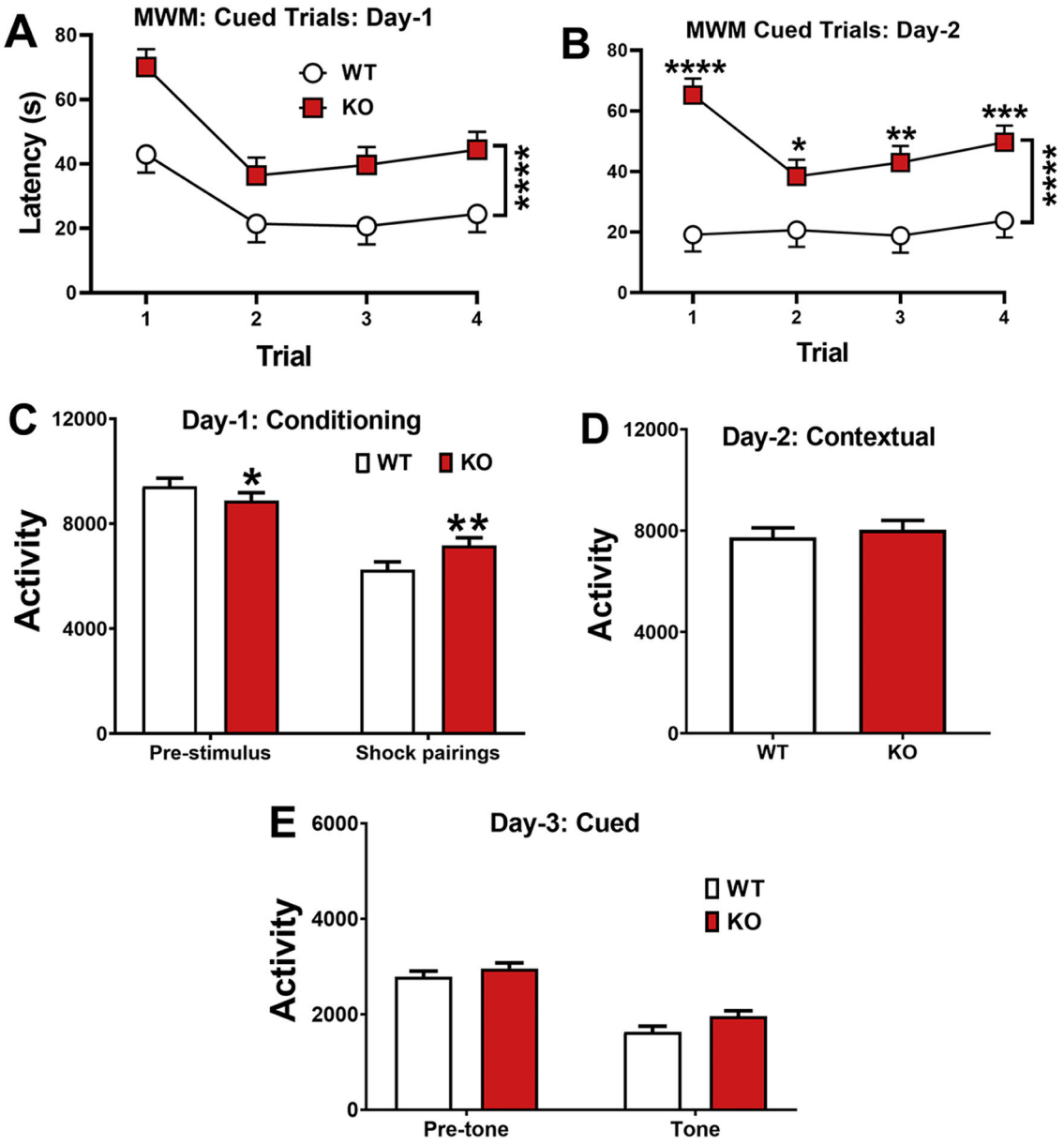

Fig. 3. Experiment-1: MWM Cued-random and Conditioned Freezing

MWM Cued trials with a visible platform and curtains closed around the maze to obscure distal cues. Start and platform positions were changed on every trial. Data are Mean ± SEM for latency, 4 trials/day for 2 days. **A**, Cued Day-1; **B**, Cued Day-2. WT n = 39 (♂ 19, ♀ 20); KO n = 40 (♂ 20, ♀ 20). Conditioned freezing: **C**, Day-1, left bars, Pre-conditioning acclimation activity (beam breaks); right bars, activity during conditioning (tone-foot-shock pairings). **D**, Day-2: Contextual memory, activity (beam breaks) in the same compartment as Day-1 (no tone or shock). **E**, Day-3: cued memory, activity (beam breaks) in a different compartment, left, before tone, right, after tone. Scale for Day-3 is different because the compartment for cued is half the size of the one used on Days 1 and 2. N are the same as for MWM Cued. Data are LS Mean ± SEM. *p<0.05, **p<0.01, ***p<0.001, ****p<0.0001 compared with WT rats.

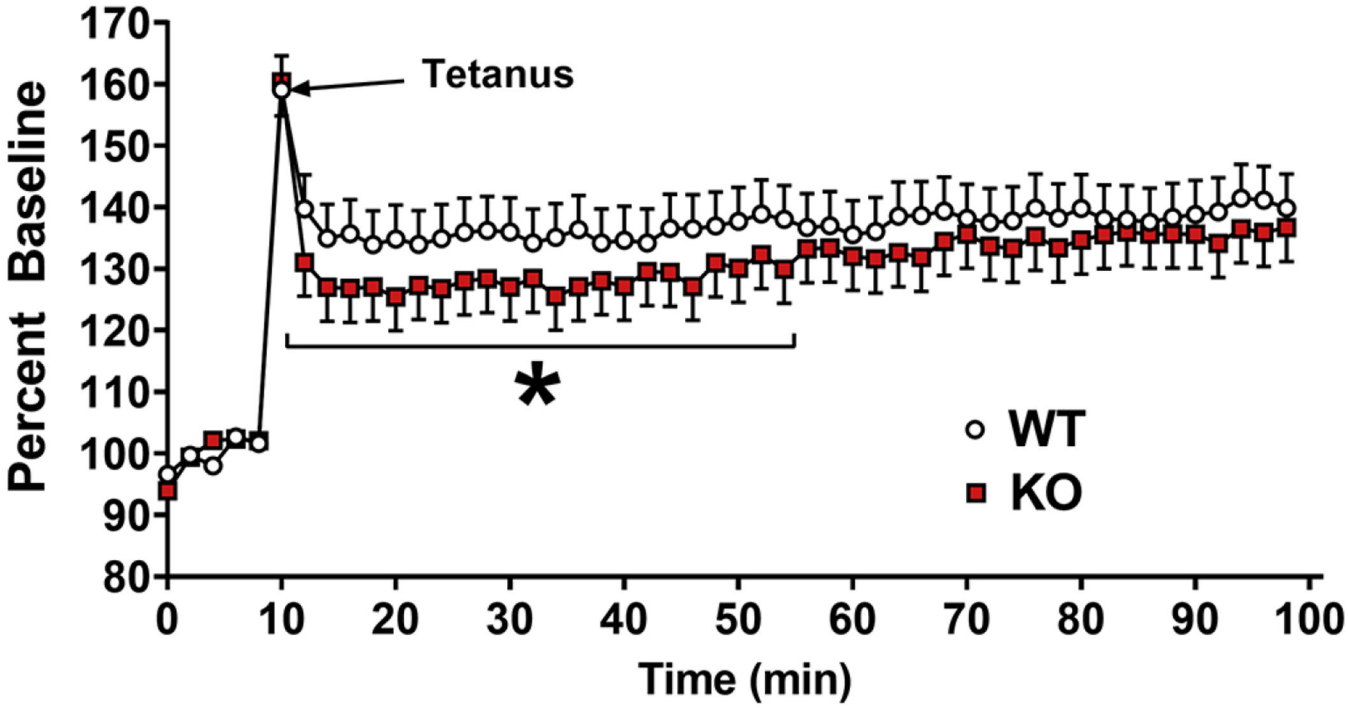

Fig. 4. Experiment-1: Long-term Potentiation (LTP)

LTP based on CA1 field fEPSP recordings and expressed as a percent of baseline. The tetanizing stimulus at arrow was tetanus = 100 Hz in 10 bursts (4 pulses/burst) delivered at a frequency of 5 Hz for 2 s delivered after 10 min of stable baseline and recorded for an additional 90 min after stimulus. WT: n = 6; KO: n = 7. *$p<0.05$ compared with WT rats.

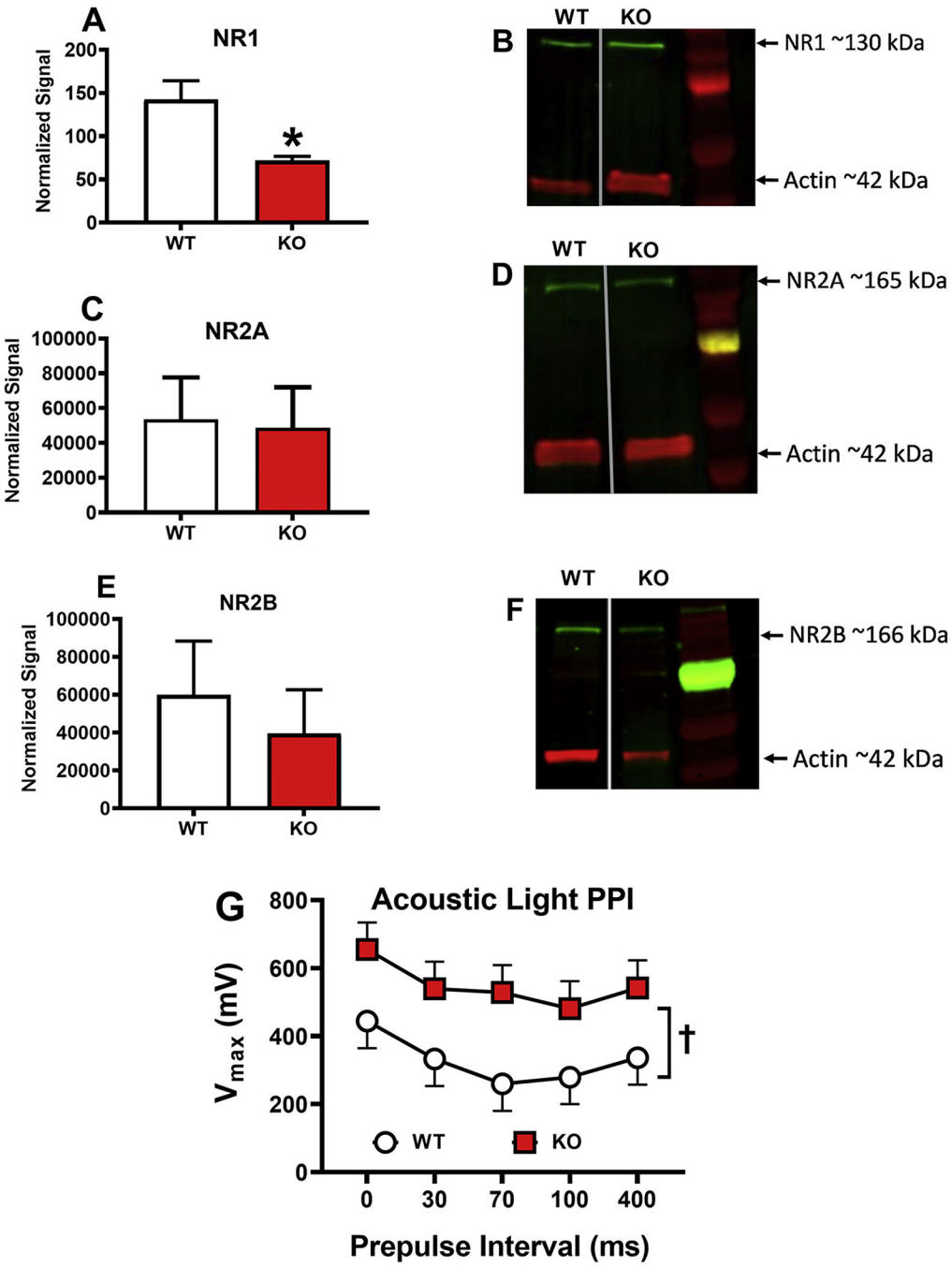

Fig. 5. Experiment-1: Hippocampal NMDA-receptor expression and prepulse inhibition of acoustic startle

Western blots of NMDA receptor subunit expression as average normalized signal; data are Mean ± SEM. **A**, NR1 levels. **B**, NR1 western blot (130 kDa). **C**, NR2A levels. **D**, NR2A western blot (165 kDa). **E**, NR2B levels. **F**, NR2B western blot (166 kDa). NMDA normalized to actin (42 kDa). WT: n = 6; KO: n = 6. **Experiment-2: Prepulse inhibition of acoustic startle with light prepulse**. **G**, Bright light prepulse inhibition of acoustic startle as a function of prepulse-to-pulse interval. WT = 10 (5 ♂ and 5 ♀); KO = 10 (5 ♂ and 5 ♀

with not more than one genotype/sex/litter. †$p<0.055$, *$p<0.05$, ***$p<0.001$ compared with WT rats.

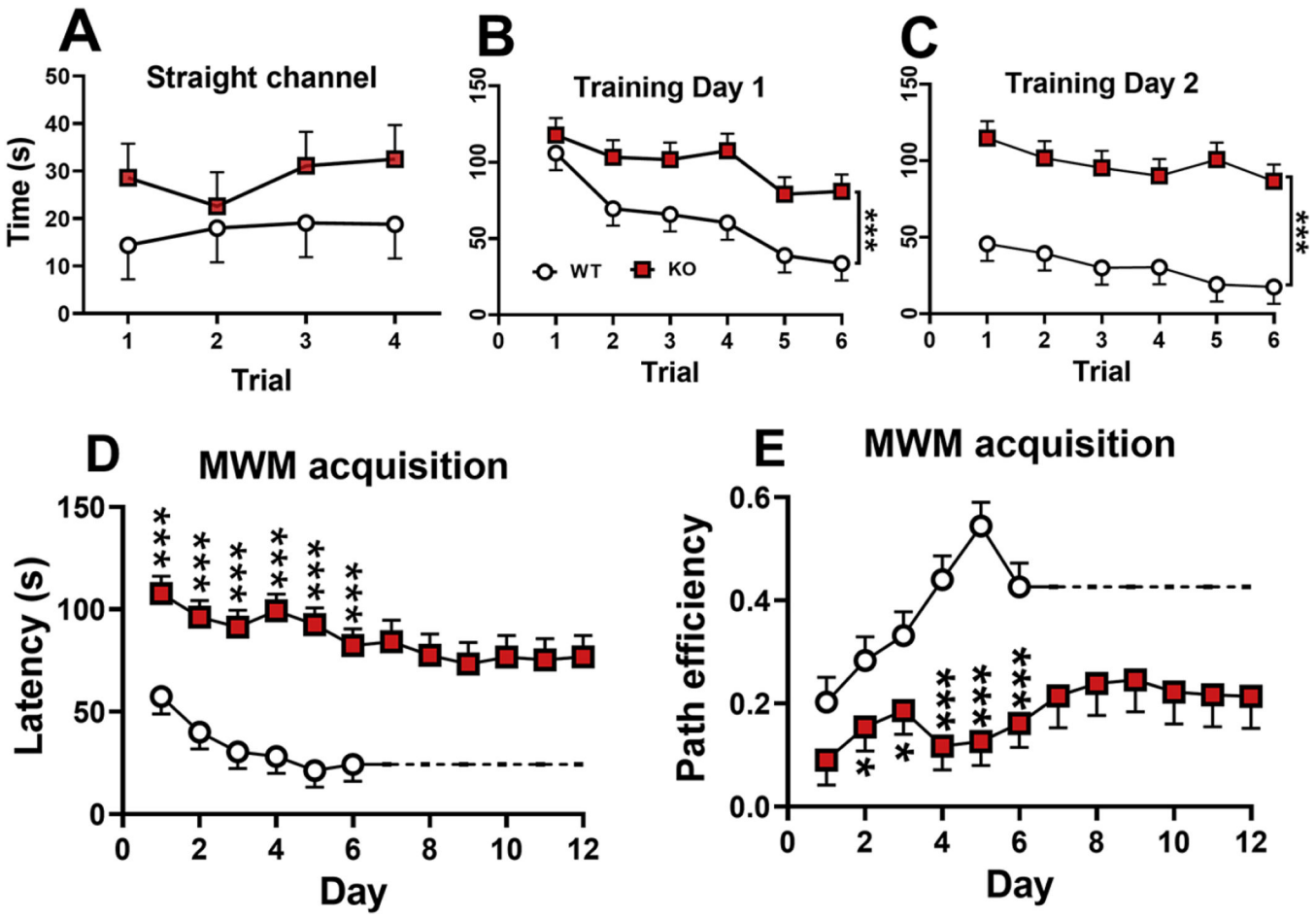

Fig. 6. Experiment-3: Morris water maze: extended acquisition (overtraining)

A, Straight channel escape latency (s). **B**, MWM training day-1 latency to a visible platform. **C**, MWM training day-2 latency to a visible platform, **D**, MWM acquisition latency to find a hidden platform, **E**, MWM path efficiency to find a hidden platform. WT n = 5 (♂ 5); KO n = 5 (♂ 5). *p<0.05; **p<0.01, ***p<0.001 compared with WT rats.

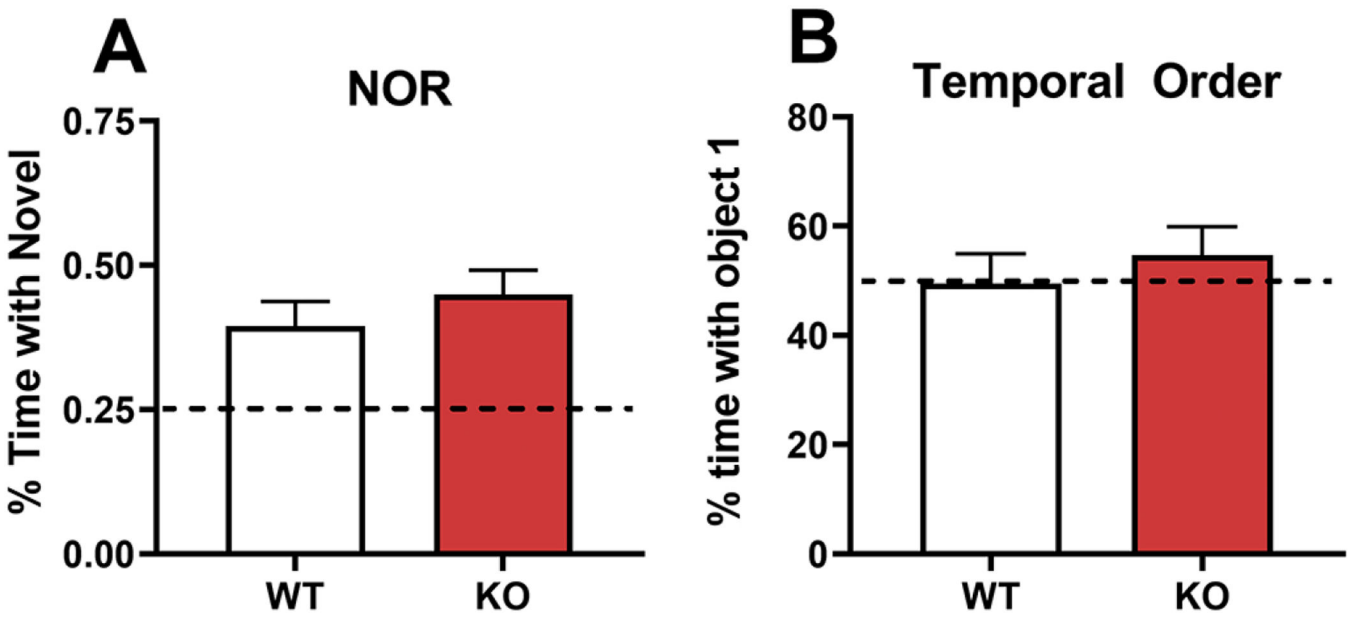

Fig. 7. Experiment-3: Novel Object Recognition and Temporal Order

Novel Object Recognition: Day-1 (familiarization): presented with 4 identical objects (one in each corner) to a criterion of attending to objects for 30 s. There were no genotype effects during familiarization (not shown). **A**, 1 h after familiarization, rats were presented with 3 identical copies of objects from day-1 plus one novel object and tested until they accumulated 30 s attending to objects. Data are percent time attending to the novel object (chance = 25%). B, Temporal Order: Step-1: Rats were presented with 2 identical objects and tested until attending to objects for a total of 30 s (not shown); Step-2: identical to day-1 except 2 different identical objects presented 4 h after Step-1 (not shown). Step-3: tested 1 h after step-2, rats presented with 1 object from step-1 and 1 object from step-2 and tested until they attended to objects for 30 s. Chance = 50%. WT n = 5 (♂ 5); KO n = 5 (♂ 5). *p<0.05; **p<0.01, ***p<0.001 compared with WT rats.

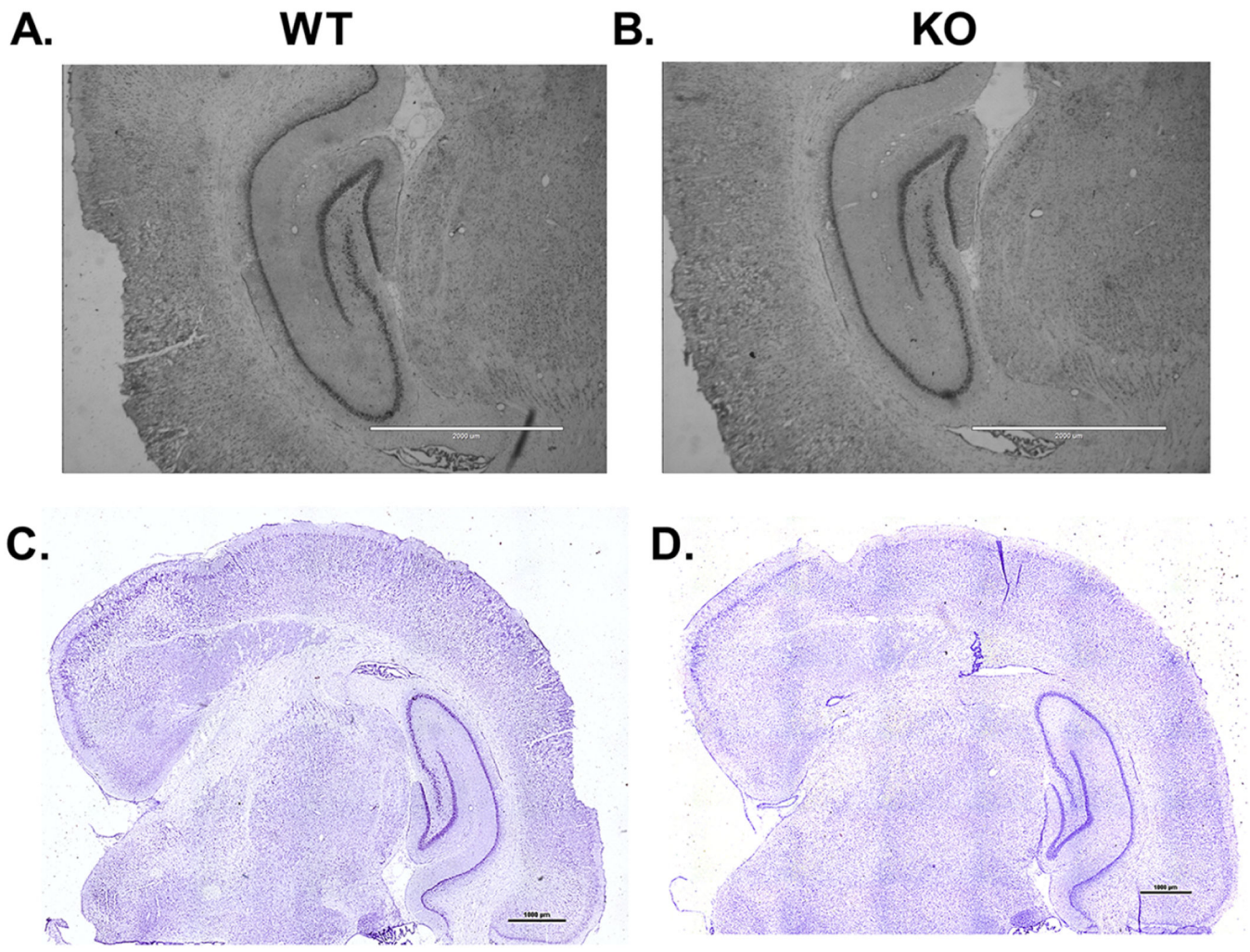

Fig. 8. Experiment-3 Histology (Nissl)

In Nissl-stained sections. No anatomical differences were observed between genotypes. Scale bar reads 1 mm. **A**, Representative image of an *Lphn3* KO rat hippocampus. **B**, Representative image of a WT rat hippocampus. 4x magnification. **C**, Large scale image of WT rat left hemisphere section. **D**, Large scale image of *Lphn3* KO rat left hemisphere section.